

All-organic PANI–DBSA/PVDF dielectric composites with unique electrical properties

Khurram Shehzad · Asad Ul-Haq · Shahabaz Ahmad · Muhamamd Mumtaz ·
Tajamal Hussain · Adnan Mujahid · Asma Tufail Shah · Muhammad Yasir Choudhry ·
Irshad Khokhar · Sadaf Ul-Hassan · Faisal Nawaz · Faiz ur Rahman ·
Yasir Butt · Muhammad Pervaiz

Received: 21 November 2012 / Accepted: 16 January 2013 / Published online: 30 January 2013
© Springer Science+Business Media New York 2013

Abstract Novel all-organic polymer high-dielectric permittivity composites of polyaniline (PANI)/poly (vinylidene fluoride) (PVDF) were prepared by solution method and their dielectric and electric properties were studied over the wide ranges of temperatures and frequencies. To improve the interface bonding between two polymers, dodecylbenzenesulfonic acid (DBSA), a bulky molecule containing a polar head and a long non-polar chain was used both as a surfactant and as dopant in polyaniline (PANI) synthesis. Synthesized conducting PANI–DBSA particles were dispersed in poly(vinylidene fluoride) (PVDF) matrix to form an all-organic composite with different PANI–DBSA concentrations. Near the percolation threshold, the dielectric permittivity of the composites at 100 Hz frequency and room temperature was as high as 170, while the dielectric loss tangent value was as low as 0.9. Like typical percolation system, composites experienced high dielectric permittivity at low filler concentrations. However, their dielectric loss tangent was low

enough to match with non-percolative ceramic filler-based polymer composites. Maximum electrical conductivity at 24 wt% of PANI–DBSA was mere 10^{-6} S/cm, a remarkably low value for percolative-type composites. Increase in the dielectric permittivity of the composites with increase in temperature from 25 to 115 °C for different PANI–DBSA concentrations was always in the same range of 50–60 %. However, the degree of increase in the electrical conductivity with the temperature was more prominent at low filler concentrations compared with high filler concentrations. Distinct electrical and their unique thermal dependence were attributed to an improved interface between the filler and the polymer matrix.

Introduction

Poly(vinylidene fluoride) PVDF, which is a flexible polymer with one of the highest dielectric permittivity of all polymers, is widely applied in many potential fields

K. Shehzad
Department of Engineering Mechanics, Centre for Nano and
Micro Mechanics, Tsinghua University, Beijing 100089, China

K. Shehzad (✉) · S. Ul-Hassan · F. u. Rahman
State Key Laboratory of Chemical Resource Engineering,
Institute of Science, Beijing University of Chemical Technology,
Beijing 100029, People's Republic of China
e-mail: khurrams@mail.tsinghua.edu.cn

A. Ul-Haq · S. Ahmad · T. Hussain · A. Mujahid ·
I. Khokhar · Y. Butt
Institute of Chemistry, University of the Punjab,
Lahore 54590, Pakistan

M. Mumtaz
Materials Research Laboratory, Department of Physics,
International Islamic University, Islamabad 44000, Pakistan

A. T. Shah
IRCBM, COMSATs Institute of Information Technology,
Lahore 54000, Pakistan

M. Y. Choudhry
Institute of Quality and Technology Management (IQTM),
University of the Punjab, Lahore 54590, Pakistan

F. Nawaz
College of Chemistry and State Key Laboratory of Inorganic
Synthesis and Preparative Chemistry, Jilin University,
Changchun 130012, China

M. Pervaiz
Department of Chemistry, Government College University,
Faisalabad, Pakistan

because of its good piezoelectric, pyroelectric response, and low acoustic impedance [1–3]. It is well known that the phase, which provide the best ferroelectric property, is one of existing PVDF crystalline phases. However, its dielectric permittivity about 6–10 is still far lower than that of non-polymer composites such as dielectric ceramics, etc. [4, 5]. For further applications as dielectric material calling for higher dielectric permittivity, it is desirable to enhance the dielectric permittivity of PVDF substantially.

A common approach for enhancing the dielectric permittivity of the polymers is to incorporate high-dielectric-constant ceramic powder, e.g., BaTiO₃ [6], PZT [7], into polymers to form a 0–3 type composites with high dielectric permittivity and low dielectric loss [8]. However, owing to the low dielectric permittivity of the polymers (i.e., $\epsilon < 10$), such polymer-based composites have relatively low dielectric permittivity (usually $\epsilon < 100$) even with high ceramic loadings (>50 vol%) [9]. Such high ceramic loadings deteriorate the mechanical properties of the composites. Thus, a key issue is to substantially raise the dielectric permittivity of polymers, while retaining their excellent mechanical properties. A common approach to achieve this goal is to use conducting fillers such as metals, carbon nanotubes, and carbon black, which utilizes the phenomenon of percolation threshold to sharply raise the electrical conductivity and dielectric permittivity of the composites at considerably low filler concentrations [10–17]. Though, these polymer percolative composites, fabricated by a combination of conductive fillers within the polymer matrix, possess a remarkably high dielectric permittivity at low filler concentrations, but their dielectric loss is also considerably high, impeding their use as effective dielectric materials. Moreover, usually the interfacial bonding between the polymer matrices and conducting fillers is not good enough. So, a mismatch of properties between filler and polymer due to poor interfacial bonding can lead to the poor mechanical properties.

Conducting polymers are relatively new class of conducting organic materials which have found widespread applications in recent times [18, 19]. These materials, being very organic in nature, offer us a unique opportunity as conducting fillers to employ them in percolative polymer composites [20–22]. They not only fulfill their role as conducting fillers but also offer excellent compatibility with polymer matrix. This compatibility not only insures the excellent mechanical properties but also give rise to unique dielectric and electric properties [23]. Polyaniline (PANI), a conducting polymer, has been employed for all-polymer percolative composites of high dielectric permittivity [24]. However, PANI when used as conducting filler is mainly doped with mineral acids, such as hydrochloric acid, sulfuric acid, etc. [21, 24, 25]. In the present work, we made an attempt to further improve the compatibility of the

PANI in the matrix polymer using an organic dopant, dodecylbenzenesulfonic acid (DBSA), a bulky molecule containing a polar head and a long non-polar chain. It was used both as a surfactant and dopant in PANI synthesis using xylene as solvent. Synthesized conducting PANI–DBSA particles were dispersed in PVDF matrix to form an all-organic composite with different PANI–DBSA concentrations. The dielectric permittivity, dielectric loss, and AC conductivity of all these composites were measured at different temperatures and frequencies.

Experimental procedures

Synthesis of PANI–DBSA

A solution of 2.9 g (0.03 M) of freshly distilled aniline, 23.5 g (0.06 M) of dodecyl benzene sulfonic acid, C₁₈H₃₀O₃S, (DBSA), and 125 ml xylene was prepared in 250-ml flask. The flask was placed in bath that was maintained at 25 °C. Polymerization was effected by the addition of an oxidant solution containing 7.1 g (0.03 M) of ammonium peroxydisulfate, (NH₄)₂S₂O₈, in 20 ml distilled water, and stirring was continued for 24 h. The molar ratio of oxidant to aniline was 1: 1 and the ratio of (DBSA) to aniline was 1:2. A dark green mixture was obtained after 24 h of polymerization. This green powder was washed with 1000 ml of water and then was washed with 450 ml of acetone until the filtrate was clear. Resulting powder was dried in oven at 50 °C for 24 h. Mechanism of PANI–DBSA synthesis is provided in Fig. 1.

Synthesis of PANI–DBSA/PVDF composites

Two gram of PVDF, 15 ml of *N,N*-dimethylformamide (DMF), and 0.08 g of PANI–DBSA was added in a flask and stirred for 12 h to obtain composites having 4 % PANI–DBSA by weight in composite. PVDF here acted as matrix material, while DMF is a solvent. Similarly, composites of PANI–DBSA/PVDF having 8, 12, 16, 20, and 24 % PANI–DBSA by weight were prepared by introducing 0.16, 0.24, 0.32, 0.4, and 0.48 g of PANI–DBSA in 2 g of PVDF. After stirring for 1 h resulting composites was casted on the glass plates and were put in the oven at 100 °C for 1 h to drive off the solvent. Films of the composites were peeled off from the glass plates and were pressed first on hot pressing machine on 15 MP for 20 min at 200 °C and then on the cold pressing machine under 15 MP pressure until sample were cooled down to the room temperature. After pressing disks of composites with different PANI–DBSA weight percent were obtained. Area of the disks was in the range of 1–1.3 cm², while thickness was in the range of 1.1–1.3 mm.

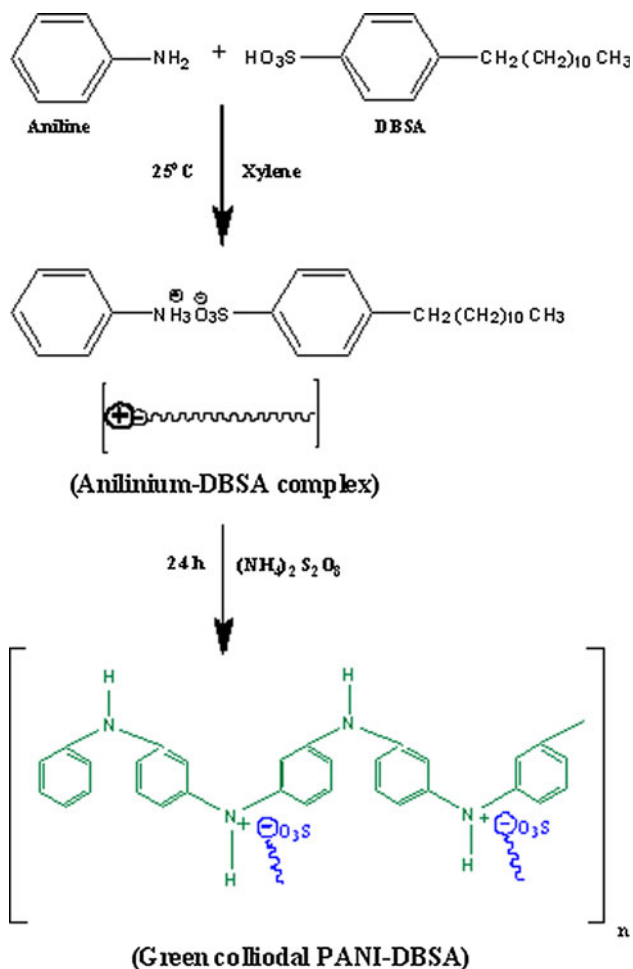


Fig. 1 Scheme of PANI-DBSA synthesis

Characterization

For the dielectric characterization, electrodes were painted on using silver paste and samples were dried at 120 °C in oven for 1 hour. The dielectric permittivity and electrical conductivity was measured between 20 and 115 °C in the frequency range of 100 Hz–10 MHz using a precision impedance analyzer (Agilent 4294A). FTIR characterization was performed on a Nicolet 5DX type instrument. Microstructure was analyzed on an environmental scanning electron microscopy (Philips-FEI XL-30).

Results and discussion

Figure 2 shows the FTIR spectra of the PANI-DBSA and PANI-DBSA/PVDF composites which shows the symmetric and anti-symmetric stretching vibrations of O = S = O and S–O groups in PANI-DBSA sample as two peaks at 1317 and 670 cm⁻¹, respectively. The peak at 1026 cm⁻¹ is due to NH₄⁺...SO⁻³ interaction between the PANI chain

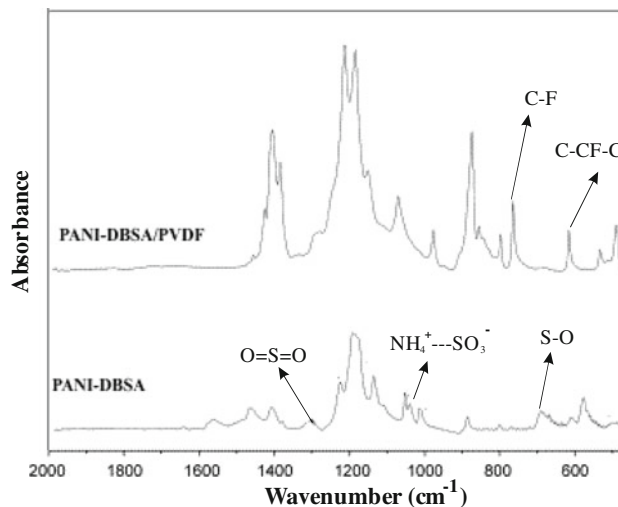


Fig. 2 The FTIR spectra of the pure PANI-DBSA and PANI-DBSA/PVDF composite

and the DBSA dopant [26]. FTIR spectra of PANI-DBSA/PVDF shows two confirming peaks of PVDF at 615 and 765 cm⁻¹ representing the CF₂ bending and the skeletal bending, respectively [27]. FTIR confirms the PANI-DBSA synthesis as well as of PANI-DBSA/PVDF composites. PANI-DBSA particles with an average size of 100 nm and electrical conductivity value of 0.5 S/cm were obtained and found to be dispersed reasonably in the PVDF matrix (Fig. 3).

Figure 4a shows the variation of dielectric permittivity of the PANI-DBSA/PVDF composite films with respect to PANI-DBSA weight percent. The dielectric permittivity of pure PVDF film was about 10. Usually, little increase in the dielectric permittivity occurs unless the concentration of conductor particles is in the neighborhood of the percolation threshold [28]. When the weight percent (wt%) or corresponding volume percent (vol%) is near the percolation threshold, the composite changes from insulator into conductor and the dielectric permittivity increases sharply. As it is shown in the Fig. 4a, there is a giant increase in dielectric permittivity of composite at 20 wt% of the filler particles. The dielectric permittivity of the composite films reached as high as 170, which is about seventeen times higher than that of the pure PVDF matrix. Interestingly, dielectric loss of the composites was comparatively low near the percolation threshold. Just below the percolation threshold (@ 16 wt%), dielectric loss tangent value of 0.06 was observed for dielectric permittivity value of 22. This combination of dielectric permittivity and dielectric loss tangent value at 16 wt% concentration of PANI-DBSA is quantitatively superior compared to some of the reported ceramic-based polymer composites. For example, reports by Dang et al. [29] and Kobayashi et al. [30] show that to obtain the dielectric permittivity value of around 25, they

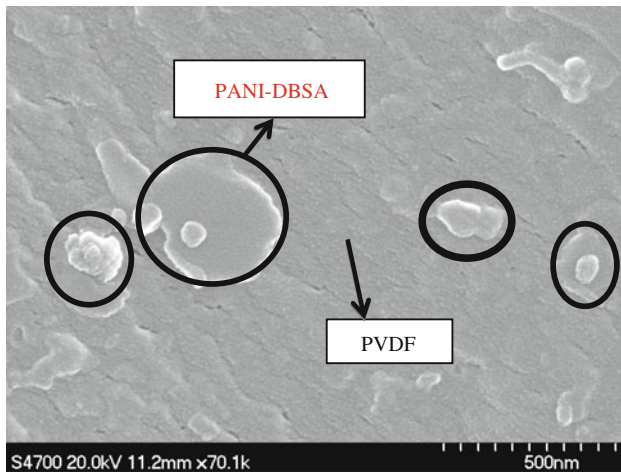


Fig. 3 Cross-sectional SEM micrograph of 20 wt% PANI-DBSA/PVDF composite

had to add BaTiO₃ inclusion of staggering 100 wt% in the PVDF matrix. Other studies show similar result where to raise the dielectric permittivity of ceramic-polymer composites to the same level of dielectric permittivity as for any PANI-DBSA inclusion level in our study, they had to use at least ten times higher weight percent of the filler [31]. One of the most important advantages to use ceramic fillers, despite their inability to raise the dielectric value, even at high filler concentration is their low dielectric loss values. Our composites not only achieved quantitatively similar dielectric values at lower filler concentrations but also our dielectric loss was low enough to be comparable with ceramic-polymer composites. Even at higher dielectric values of 78 and 170, respective dielectric loss tangent was at very reasonable values of 0.36 and 0.9, respectively. Though, the dielectric loss tangent values when compared with low concentrations of PANI-DBSA, was high for dielectric value of 170, but it still was far lower when compared to other conducting filler-based composites where dielectric loss tangent was extremely high near the percolation threshold [28]. In fact, our PANI-DBSA/PVDF composites had a unique synergy where they combined the “high dielectric permittivity at low concentration” characteristics of percolative composites with “low dielectric

loss at high dielectric permittivity” characteristics of ceramic-polymer composites. Apart from superior dielectric values at low filler concentrations for our composites, another added advantage over ceramic-polymer composites and the other conducting filler-based composites is that the use of organic filler in current study will certainly insure the better mechanical properties. Near the percolation threshold the increase in dielectric permittivity of PANI-DBSA/PVDF composites with increase in filler concentration can be explained by the following power law:

$$\varepsilon = \varepsilon_0 [(f_c - f)/f_c]^{-q} \quad (1)$$

where ε_0 is the dielectric permittivity of insulator matrix, f is the volume fraction of conductive particles, f_c is the percolation threshold, and q is a critical exponent. As Fig. 4 shows the value of f_c was 0.27 corresponding to 20 wt%, while value of q was 0.48. The value of exponent q is much lower than the universal value of 1 [32], which might hint a non-universal behavior of composites below percolation threshold. Volume fraction from weight percent can be calculated by density value of PANI-DBSA (1.32 g/cm³) and PVDF (1.78 g/cm³). The increment in dielectric permittivity of PANI-DBSA/PVDF composites could mainly be ascribed to Maxwell-Wagner (MW) polarization originating at the insulator-conductor interfaces [33]. In fact, the increase of dielectric permittivity as well as electrical conductivity can also be comprehended by assessing the gradual formation of microcapacitor networks in the PANI-DBSA/PVDF composite film with the increase in concentration of PANI-DBSA. As shown in schematics of Fig. 5, below the percolation threshold, the filler particles remain in isolation, and only few short-range conducting paths exist. However, as weight percent of PANI-DBSA particles approached near the percolation threshold, scattered particles of filler came such close that inter-particle distance was short enough to make a continuous path or network resulting in sudden increase in the dielectric permittivity. Main mechanism of electrical transport near percolation threshold in such polymer composites where conducting fillers are separated by a thin insulating layer of polymers is tunneling. However, for

Fig. 4 Dependence of **a** dielectric permittivity **b** electrical conductivity on PANI-DBSA concentrations at room temperature and 100 Hz frequency

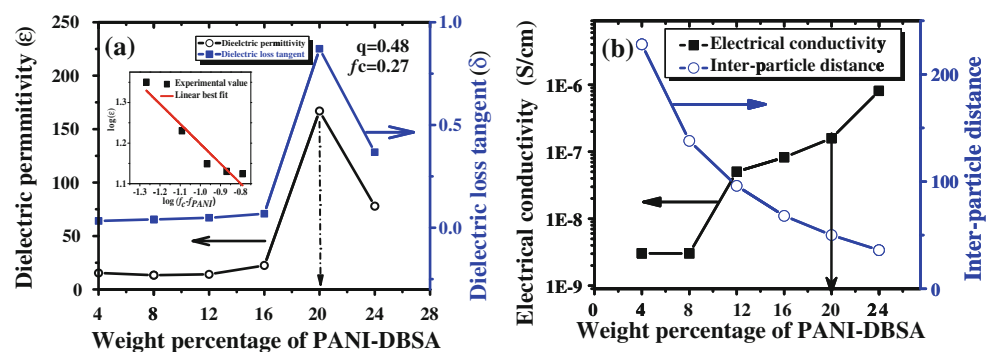
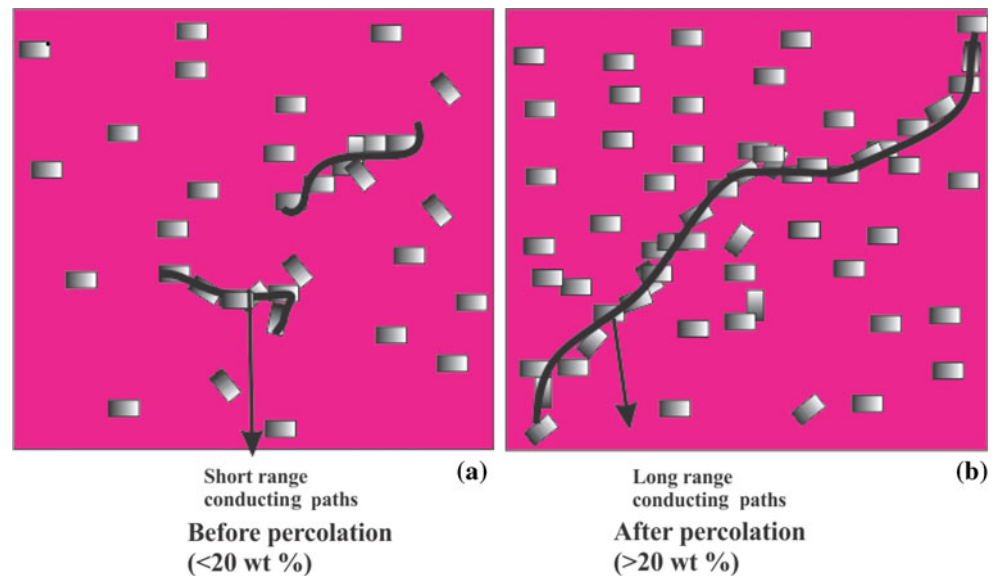


Fig. 5 Schematic depiction of the microstructure of the all-organic PANI–DBSA/PVDF composite **a** with PANI–DBSA <20.0 wt%, and **b** with PANI–DBSA >20.0 wt%



tunneling to occur inter-particle distance for ideally dispersed particles must be in the range of few nanometers, <1.8 nm exactly [34]. One can calculate the inter-particle distance from a simple relation $S = d[(\pi/6f)-1]$ [35], where d is diameter of filler particles, which in this case had an average value of 100 nm, f is the filler volume fraction, and π is a constant. However, as no filler is ideally dispersed and distributed; so theoretically, when calculated for percolation threshold, tunneling distance will always yield a higher than 1.8-nm tunneling distance. By means of the above-mentioned relation, we found the inter-particle distance values of 228, 138, 96, 68, 50, and 36 nm for 4, 8, 16, 20, and 24 wt% of filler, respectively. As obvious inter-particle distance decreased exponentially (See Fig. 4b) with filler concentration and increase in dielectric constant was also exponential. Percolation threshold was found to be at the inter-particle distance of 68 nm at 20 wt%, which was considerably longer than the maximum inter-particle distance of 1.8 nm required for the tunneling to occur. Appearance of percolation despite the mismatch between the inter-particle distance at 20 wt% (68 nm) and the maximum inter-particle distance allowed (1.8 nm) for tunneling process hints the non-ideal dispersion patterns. Electrical conductivity in previous reports is also shown to experience the same exponential increase near the critical filler concentration as the dielectric permittivity [36, 37]. However, as shown in Fig. 4b, remarkably, in our composites not only the increase in electrical conductivity was marginal ($10^{-9} \rightarrow 10^{-6}$ S/cm) but also increase never experienced a classical percolation-like feature. In fact, the conductivity-concentration curve shared the features of semi-conducting fillers. There was a small jump ($\sim 10^{-9} \rightarrow \sim 10^{-7}$ S/cm) in electrical conductivity at 12 wt%, but in the vicinity of the percolation, remarkably,

electrical conductivity experienced a smooth gradual increase. We believe this low conductivity at percolation threshold that arises from better compatibility between filler and polymer is main reason for low dielectric loss of the PANI–DBSA/PVDF composites. Low electrical conductivity and unique conductivity-filler concentration curve might have been result of better compatibility between matrix and filler polymers which resulted in a diffused interface between them, hindering the flow of charges in conducting filler networks, producing low conductivity values, even near the percolation threshold. One of the major drawbacks, percolative dielectric composites suffer from, is a high electrical conductivity value near the percolation threshold. Higher conductivity can lead to higher leakage current and higher dielectric loss. Extremely low percolation conductivity (10^{-7} S/cm) as well as the low post-percolation conductivity (10^{-6} S/cm) at the concentration of 24 wt% is an important feature of our composites. It is also worth highlighting that low dielectric loss and low electrical conductivity is required criteria for high dielectric strength, and our composites fulfilled this criterion.

Anomalously low electrical conductivity values and unique quasi-linear conductivity curve may question the presence of MW polarization and percolation phenomenon in the composites. If the MW polarization, viz, the space charge polarization and percolation plays an important role in the dielectric response of PANI–DBSA/PVDF percolation system, it will lead to strong dependence of the dielectric permittivity on THE frequency, especially in low frequency range. It is clear from the Fig. 6a that in the region where the weight percent was less than percolation threshold, dependence of the dielectric permittivity on the frequency was very weak. However, when the weight

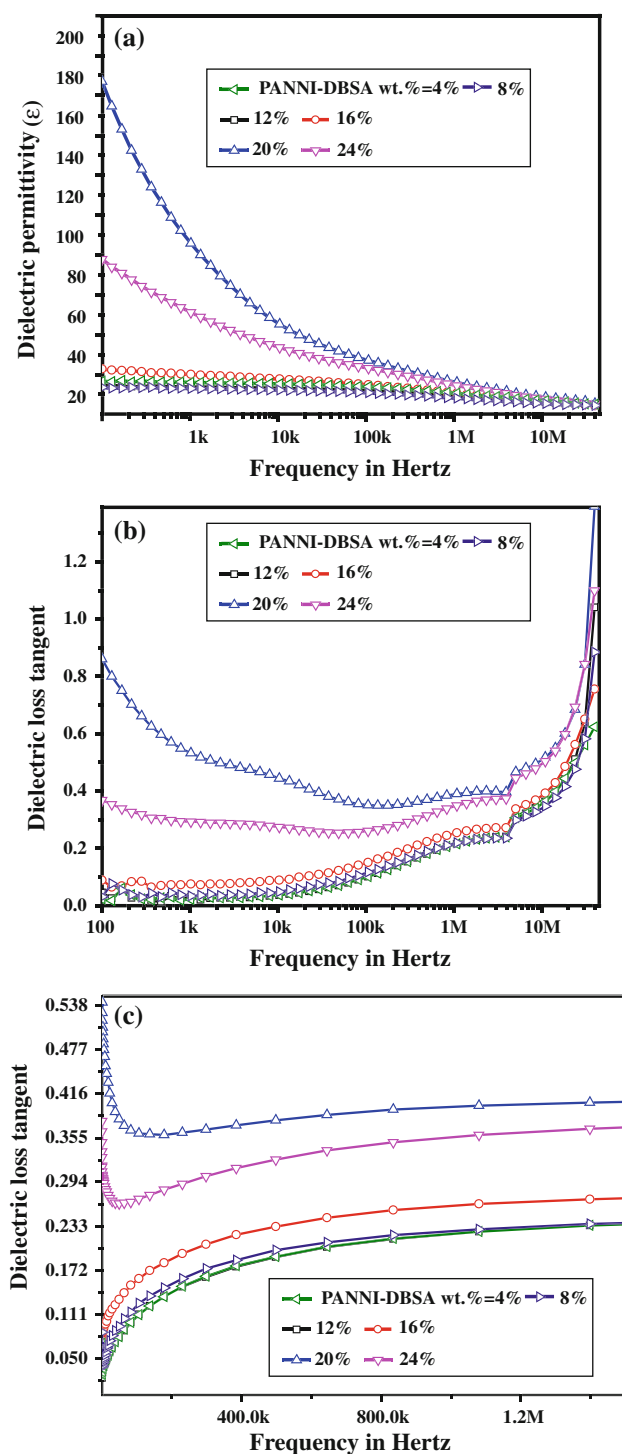


Fig. 6 Dependence of the **a** dielectric permittivity **b, c** dielectric loss tangent of PANI-DBSA/PVDF composites with different amounts of PANI-DBSA inclusions on the frequency at the room temperature

percent of PANI-DBSA was at or greater than the percolation threshold, a strong dependence of dielectric permittivity on the frequency, especially in the low frequency range ($<10^4$ Hz), was clearly visible, confirming the MW polarization and percolation phenomenon [38]. Dielectric

loss tangent of composites in Fig. 6b, c, at lower frequencies (<400 kHz) and higher frequencies (>400 kHz), anomalously, presented a contrasting behavior for pre- and post-percolation threshold composites. However, at very high frequencies (>100 k) there was a convergence of frequency dependence for both pre- and post-percolation threshold composites.

The dependence of dielectric permittivity, PANI-DBSA/PVDF composites on the weight percent of PANI-DBSA, at different temperatures is shown in the Fig. 7a, b. It can clearly be seen over the whole weight range, even in the neighborhood of the percolation threshold, the dielectric permittivity presented an augmented response with the increase in temperature from 25 to 115 °C. When the temperature was at 115 °C, the dielectric permittivity reached as high as 231, indicating an increase of nearly 60 % from dielectric value of 148 at 25 °C. Remarkably, for every PANI-DBSA concentration in our study the increase in the dielectric permittivity from 25 to 115 °C was always in the range of 50–60 %. This uniform increase for all the PANI-DBSA concentrations despite different initial dielectric permittivity values is inconsistent with already reported results that show a greater increase in the dielectric permittivity with increasing temperature for the concentrations near the percolation threshold [39]. Furthermore, particle fillers like PANI-DBSA are bound to show drop in the dielectric permittivity and the electrical conductivity as particle filler networks always breakdown due to thermally induced volume expansion of the matrix polymer [36]. But, in this case, dielectric permittivity and also, as shown in Fig. 8a, the electrical conductivity of the composites increased with the temperature. Interestingly, in contrast with dielectric permittivity, electrical conductivity experienced a different degree of dependence for different concentrations of PANI-DBSA. For example, the electrical conductivity of the composites with 4 wt% of PANI-DBSA at 115 °C is nearly an order of magnitude higher than at 25 °C. This scale of increase in electrical conductivity is unmatched not only for pure PVDF but also for other PANI-DBSA-loaded composites. Dependence of the electrical conductivity on the temperature at higher PANI-DBSA concentrations (in the vicinity of the percolation threshold) was very weak, demonstrating different degree of electrical conductivity dependence on the temperature at low and high PANI-DBSA concentrations. The temperature-enhanced dielectric permittivity and conductivity of the composites with different amounts of PANI-DBSA inclusions, especially below the percolation threshold is due to specific microstructure of the composite with particular PANI-DBSA loading, schematically illustrated in Fig. 2. It is widely accepted that when the concentration of the conductive phase is lower than the percolation threshold, the enhancement in conductivity can be explained by the inter-particle tunneling effect. Such tunneling occurs when the effective tunneling range of two fillers

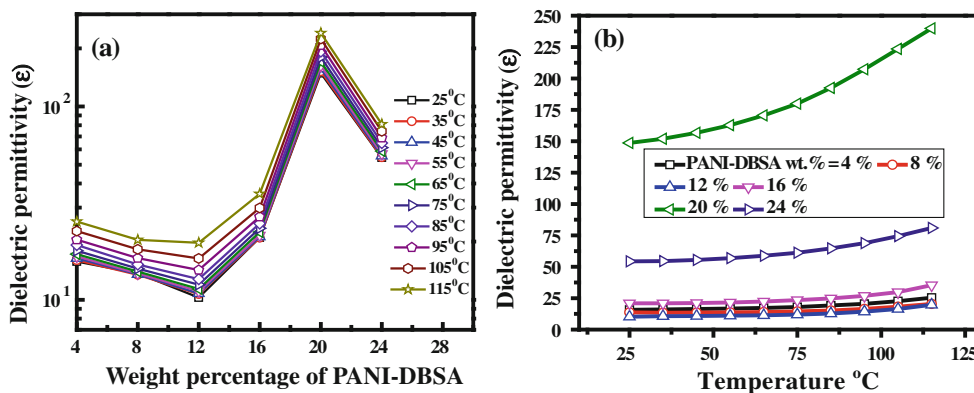


Fig. 7 a, b Dependence of the dielectric permittivity for the PANI–DBSA/PVDF composites on the weight percentage of PANI–DBSA and different temperatures at 100 Hz AC frequency

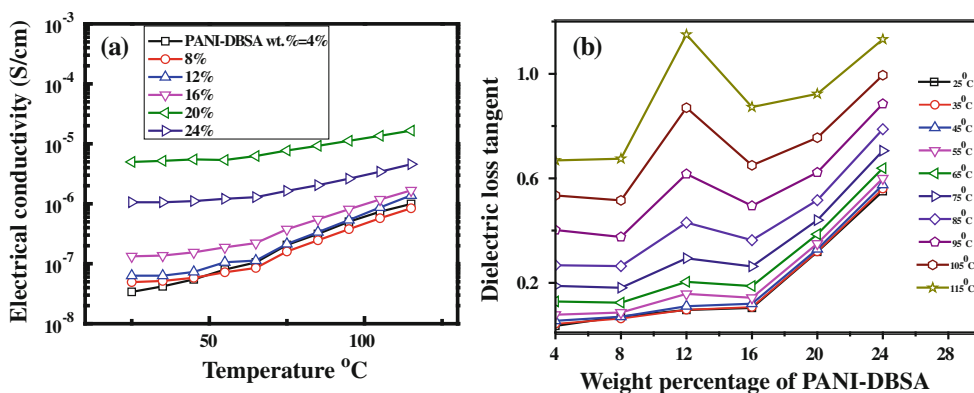


Fig. 8 a Dependence of the electrical conductivity b dielectric loss tangent for the PANI–DBSA/PVDF composites on the weight percentage of PANI–DBSA and different temperatures measured at 100 Hz AC frequency

overlaps. This tunneling effect weakens if the gap between the filler particle is large. Enhanced compatibility between PANI and DBSA and the PVDF avoided the large gaps between the fillers at higher temperature and allowed the tunneling range to overlap at all temperatures. This lead to the strong enhancement in both dielectric permittivity and conductivity due to the emergence of the more efficient percolative path with increasing temperature, as the inter-particle tunneling is a thermally activated process. Figure 8b shows the dielectric loss behavior of different composite at different temperatures. A sharp increase in dielectric loss was observed at PANI–DBSA concentration of 12 wt%. Increase was not prominent at and above the percolation threshold. Dielectric loss at higher temperature for 12 wt% PANI–DBSA was even higher than the dielectric loss at the percolation threshold. Possible explanation lies in start of the aggregation process for PANI–DBSA particles in the matrix polymers to form conductive networks. This hypothesis is supported by a jump in the electrical conductivity at 12 wt% PANI–DBSA concentrations in Fig. 4b.

Conclusion

Results indicate that PANI–DBSA acted as a novel filler to achieve the PVDF-based composite with high dielectric permittivity, low dielectric loss, and low electrical conductivity. These properties come from better compatibility between PVDF and PANI–DBSA. Increase in dielectric permittivity with the temperature was on the same scale for all the PANI–DBSA filler concentrations. However, increase in electrical conductivity for the composites with low concentration of PANI–DBSA was the most significant. The tunneling effect between filler particles and microstructure resulting from enhanced compatibility between PVDF and PANI–DBSA was responsible for such unique dependence of the electrical properties on the temperature. These PANI–DBSA/PVDF composites due to their unique dielectric and electrical properties can find applications as energy storage materials for variety of commercial uses.

References

1. Stolichnov I, Maksymovych P, Mikheev E, Kalinin SV, Tagantsev AK, Setter N (2012) *Phys Rev Lett* 108:27603
2. Li W, Meng Q, Zheng Y, Zhang Z, Xia W, Xu Z (2010) *Appl Phys Lett* 96:192905
3. Zhong Z, Cao Q, Jing B, Wang X, Li X, Deng H (2012) *Mater Sci Eng B* 177:86. doi:10.1016/j.mseb.2011.09.008
4. Vangchangyia S, Swatsitang E, Thongbai P et al (2012) *J Am Ceram Soc* 95:1497. doi:10.1111/j.1551-2916.2012.05147.x
5. Dang ZM, Zhou T, Yao SH et al (2009) *Adv Mater (Weinheim Ger)* 21:2077
6. Dang ZM, Yu YF, Xu HP, Bai J (2008) *Compos Sci Technol* 68:171
7. Zak A, Gan W, Majid W, Darroudi M, Velayutham T (2011) *Ceram Int* 37:1653
8. Choi Y, Yoo M-J, Kang H-W, Lee H-G, Han S, Nahm S (2012) *J Electroceram* 1. doi:10.1007/s10832-012-9706-7
9. Dang ZM, Lin YQ, Xu HP, Shi CY, Li ST, Bai J (2008) *Adv Funct Mater* 18:1509
10. Dang ZM, Shehzad K, Zha JW, Hussain T, Jun N, Bai J (2011) *Jpn J Appl Phys* 50:0214
11. Dang Z-M, Shehzad K, Zha J-W et al (2011) *Compos Sci Technol* 72:28. doi:10.1016/j.compscitech.2011.08.020
12. Sahoo B, Naskar K, Dubey K, Choudhary R, Tripathy D (2012) *J Mater Sci* 47:2421. doi:10.1007/s10853-012-6782-7
13. Yao SH, Dang ZM, Jiang MJ, Xu HP, Bai J (2007) *Appl Phys Lett* 91:212901
14. Yao SH, Dang ZM, Xu HP, Jiang MJ, Bai J (2008) *Appl Phys Lett* 92:082902
15. Yao SH, Yuan JK, Zhou T, Dang ZM, Bai J (2011) *J Phys Chem C* 115:20011
16. Shehzad K, D Zhimin, MN Ahmad et al. (2012) *Carbon*. doi: <http://dx.doi.org/10.1016/j.carbon.2012.10.068>
17. Zha J-W, Shehzad K, Li W-K, Dang Z-M (2013) *J Appl Phys* 113:014102
18. Shang S, Wei Z, TAO X (2012) *RSC Adv* 2:4675
19. Fang FF, Liu YD, Lee IS, Choi HJ (2011) *RSC Adv* 1:1026
20. Huang C, Zhang Q (2004) *Adv Funct Mater* 14:501
21. Huang C, Zhang Q, Debotton G, Bhattacharya K (2004) *Appl Phys Lett* 84:4391
22. Zhou T, Zha JW, Hou Y, Wang D, Zhao J, Dang ZM (2011) *ACS Appl Mater Interfaces* 3:4557
23. Yuan JK, Dang ZM, Yao SH et al (2010) *J Mater Chem* 20:2441
24. Huang C, Zhang Q, Su J (2003) *Appl Phys Lett* 82:3502
25. He X, Du J, Ying Z, Cheng H (2005) *Appl Phys Lett* 86:062112
26. Babazadeh M (2009) *J Appl Polym Sci* 113:3980
27. Bormashenko Y, Pogreb R, Stanevsky O, Bormashenko E (2004) *Polym Test* 23:791. doi:10.1016/j.polymertesting.2004.04.001
28. Dang ZM, Wang L, Yin Y, Zhang Q, Lei QQ (2007) *Adv Mater* 19:852. doi:10.1002/adma.200600703
29. Dang ZM, Xie D, Shi CY (2007) *Appl Phys Lett* 91:222902
30. Kobayashi Y, Tanase T, Tabata T, Miwa T, Konno M (2008) *J Eur Ceram Soc* 28:117. doi:10.1016/j.jeurceramsoc.2007.05.007
31. Deng Y, Zhang Y, Xiang Y, Wang G, Xu H (2009) *J Mater Chem* 19:2058
32. Ce-Wen N (1993) *Prog Mater Sci* 37:1
33. Chanmal C, Jog J (2012) *Characterization Techniques for Polymer Nanocomposites*: 167
34. Li C, Thostenson ET, Chou TW (2007) *Appl Phys Lett* 91: 223114
35. Dang ZM, Yuan JK, Zha JW, Zhou T, Li ST, Hu GH (2012) *Prog Mater Sci* 57:660
36. Xu HP, Dang ZM, Bing NC, Wu YH, Yang DD (2010) *J Appl Phys* 107:034105
37. Xu HP, Dang ZM (2007) *Chem Phys Lett* 438:196
38. Pötschke P, Dudkin SM, Alig I (2003) *Polymer* 44:5023
39. Wang L, Dang ZM (2005) *Appl Phys Lett* 87:042903